Available online at www.sciencedirect.com
ScienceDirect
Journal of Magnetic Resonance 189 (2007) 13–19
JMR Journal of Magnetic Resonance
www.elsevier.com/locate/jmr

High resolution ^{1}H NMR of a lipid cubic phase using a solution NMR probe

E. Boyle-Roden [a], N. Hoefer [b], K.K. Dey [a], P.J. Grandinetti [a,*], M. Caffrey [b]

[a] Department of Chemistry, The Ohio State University, 120 W. 18th Avenue, Columbus, OH 43210-1173, USA
[b] Department of Chemical and Environmental Sciences, University of Limerick, Limerick, Ireland

Received 9 March 2007; revised 8 August 2007
Available online 22 August 2007

Abstract

The cubic mesophase formed by monoacylglycerols and water is an important medium for the *in meso* crystallogenesis of membrane proteins. To investigate molecular level lipid and additive interactions within the cubic phase, a method was developed for improving the resolution of ^{1}H NMR spectra when using a conventional solution state NMR probe. Using this approach we obtained well-resolved *J*-coupling multiplets in the one-dimensional NMR spectrum of the cubic-Ia3d phase prepared with hydrated monoolein. A high resolution *t*-ROESY two-dimensional ^{1}H NMR spectrum of the cubic-Ia3d phase is also reported. Using this new methodology, we have investigated the interaction of two additive molecules, L-tryptophan and ruthenium-tris(2,2-bipyridyl) dichloride (rubipy), with the cubic mesophase. Based on the measured chemical shift differences when changing from an aqueous solution to the cubic phase, we conclude that L-tryptophan experiences specific interactions with the bilayer interface, whereas rubipy remains in the aqueous channels and does not associate with the lipid bilayer.

Keywords: Crystallization; Membrane proteins; Mesophase; Nuclear magnetic resonance

1. Introduction

Hydrated lipids can exist in a variety of liquid crystalline or mesophases depending on temperature and sample composition (Fig. 1). One of these, the lamellar phase (Fig. 1B), has long and successfully been used as a model for the lipid component of the biological membrane. A second liquid crystalline phase, the cubic phase, has gained notoriety as a host for membrane protein crystallization by the so-called *in meso* method [1,2]. It has also been used in controlled release and uptake studies [3,4] and is of interest as an intermediate in membrane fusion [5] and fat digestion [6]. The lipid component of the bicontinuous cubic phase takes the form of a highly curved, continuous bilayer that permeates three-dimensional space as a set of connected saddle sections. The bilayer divides the aqueous component into two branched networks of channels. The channels interpenetrate but never contact one another because of the intervening bilayer (Fig. 1C and D). The midplane of the bilayered membrane describes a periodic minimal surface where mean curvature is everywhere zero [7,8].

An intriguing aspect of the highly viscous cubic phase is its NMR[1] spectrum, which, unlike the lamellar phase, does not exhibit anisotropic broadening. Molecules laterally diffusing parallel to its periodic minimal surface [8] reorient with a symmetry [9] that eliminates second rank NMR frequency anisotropies such as chemical shift anisotropy and hetero- and homonuclear dipolar couplings. It has long been known that ^{13}C and ^{31}P NMR spectra of the cubic phase exhibit narrow, resolved peaks [10–12]. More

* Corresponding author. Fax: +1 614 292 1685.
E-mail address: grandinetti.1@osu.edu (P.J. Grandinetti).

[1] *Abbreviations:* MAS, magic-angle spinning; MPDB, membrane protein data bank; NMR, nuclear magnetic resonance, rubipy, ruthenium-tris (2,2-bipyridyl) dichloride; PDB, protein data bank, DSS, 2,2-dimethyl-2-silapentane-5-sulfonate sodium salt; SAXS, small-angle X-ray scattering.

1090-7807/$ - see front matter © 2007 Elsevier Inc. All rights reserved.
doi:10.1016/j.jmr.2007.08.010

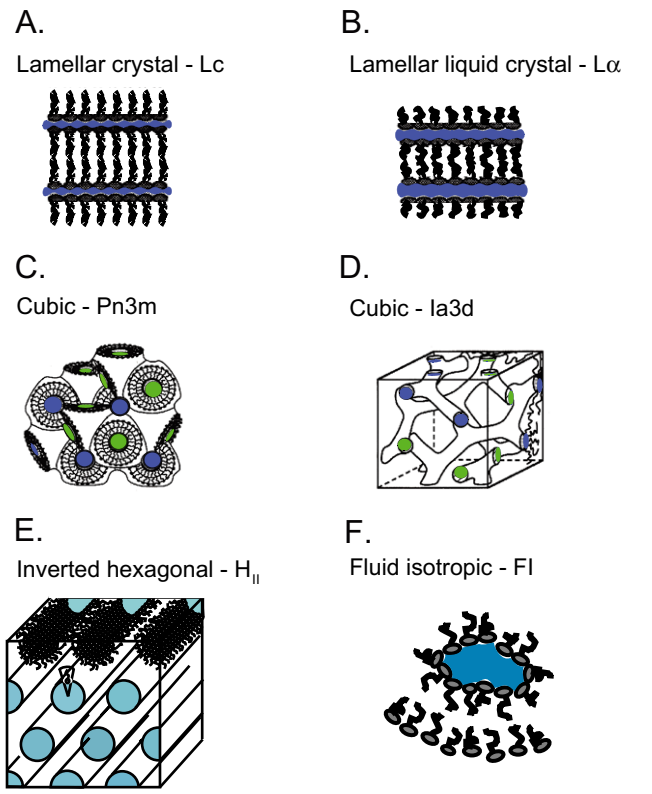

Fig. 1. Cartoon representation of the various mesophases formed by monoolein and water. Individual lipids are shown as lollipop figures with the pop and stick parts representing the polar head groups and the apolar acyl chain, respectively. The colored regions represent water. (For interpretation of the references to colour in this figure legend, the reader is referred to the web version of this article.)

recently, it has been shown [13–16] that the cubic phase eliminates strong homonuclear proton dipolar couplings and that high resolution ^{1}H NMR spectra can be obtained with magic-angle spinning (HR-MAS) [13], which further removes the residual spectral broadening that arises from bulk magnetic susceptibility variations. These susceptibility variations arise because the highly viscous nature of the cubic phase makes it difficult to load sample containers, such as conventional solution state NMR tubes, without introducing air bubbles and other inhomogeneities. Conversely, a sample free of bubbles will only produce susceptibility broadening at the boundaries of the sample with the tube that contains it and the air that surrounds the tube. Forcing the cubic phase to assume the shape of a long (nearly infinitely long) cylindrical tube will therefore eliminate the "end effects" and produce a uniform demagnetization field [17,18]. Here, we show that high resolution ^{1}H NMR spectra with resolved *J*-coupling multiplets can be obtained using a conventional liquid state NMR probe, without HR-MAS, by loading uniform and homogenous samples of the high viscosity cubic phase into thin-walled glass capillaries. Not only does this approach make high resolution NMR studies in the cubic phase more accessible it also avoids potential sample heating effects of MAS, permits more precise temperature control and enables both X-ray diffraction and NMR spectroscopic measurements to be performed on the same sample. Additionally, we examine the ^{1}H NMR spectra of two molecules, L-tryptophan and ruthenium-tris(2,2-bipyridyl) dichloride (rubipy), with varying diffusional release rates from the cubic phase to assess potential differences in the interaction of these molecules with the lipid component of the bilayer.

2. Materials and methods

2.1. Materials

Monoolein was purchased from Nu Chek Prep. Inc. (Elysian, MN). 99.96% D_2O was obtained from Cambridge Isotope Labs (Andover, MA). Syringes were from Fisher Scientific (Hamilton 81030, 100 μL gas-tight). Water, with a resistivity of >18 MΩ-cm, was purified by a Milli-Q Reagent Water System, (Millipore Corporation, Bedford, MA) containing a carbon filter cartridge, two ion-exchange filter cartridges, an organic removal cartridge and a final 0.2 μm filter (Sterile Millipore millipak 40, lot F2PN84024). Rubipy was kindly provided by Dr. Claudia Turro (The Ohio State University). 2,2-Dimethyl-2-silapentane-5-sulfonate sodium salt (DSS) was purchased from Aldrich (St. Louis, MO; lot #17216EB). L-tryptophan(lot #119HO3-LL) was from Sigma (St. Louis, MO).

2.2. Sample preparation

Samples of fixed hydration were prepared by mechanical mixing of appropriate amounts of lipid and aqueous solution to achieve the desired overall sample composition of 63%(w/w) lipid. Homogenization was accomplished at room temperature (20–22 °C) by cycling the lipid/aqueous mixture at least 60 times between two 100 μL microsyringes (Hamilton Company, Reno, NV) through a short (6 mm) 22-gauge coupling needle, as described [19]. The homogenized material was loaded into 3 cm long, 1.0 mm diameter (0.01 mm wall thickness) glass capillaries (Charles Supper Natick, MA). Transfer with minimal water loss was accomplished by uncoupling the lipid mixer and attaching a standard 22-gauge needle to the syringe containing the sample. This was used to place the mesophase in the capillary. Particular care was taken to withdraw the capillary from the tip of the syringe needle during the filling process to ensure uniform, bubble-free loading. This procedure avoids the need for prolonged high-speed centrifugation. Capillaries were flame sealed (Model 6, Microflame, Inc., Minnetonka, MN), glued with 5 min epoxy (Hardman Inc., Belleville, NJ) and stored for up to 7 days at room temperature prior to data collection. Incorporation of L-tryptophan or rubipy into the cubic phase was achieved by using a solution of the corresponding additive in water or D_2O to hydrate the lipid in the initial mixing process. The solution concentrations of additives were tryptophan, 8 mg/mL; and rubipy, 10 mg/mL. Final molar ratios of additive to lipid in the cubic phase samples were: tryptophan, 1:122; and rubipy, 1:166.

2.3. X-ray diffraction

Phase identity and microstructure of the sample was determined by small-angle X-ray diffraction (SAXS) using point focused Cu-K_α X-rays (1.542 Å, nickel (0.025 mm-thick) filtered) produced using a two-beam port Rigaku RU-300 18 kW rotating anode generator (Rigaku USA, Inc., Danvers, MA) operated at 40 kV and 200 mA. Static diffraction patterns were collected at 20 °C. Exposure times were 30–60 min at a sample-to-detector distance of 24–34 cm. Samples were examined under cross-polarized light with a Nikon Eclipse E400 microscope at 10× and 40× magnification to confirm that the region of interest within the capillary was uniformly in the cubic phase.

The diffraction measurements show that the samples used in this study were in the cubic-Ia3d phase in agreement with the known phase behavior of monoolein at 20 °C (see Fig. 1 in reference [20]). The lattice parameter of the mesophase ranged from 127 to 150 Åover the course of the study. This variation is due primarily to slight differences in the water content of the samples, which have a nominal value of 37%(w/w). When additives were included in the sample, SAXS was used to evaluate the phase state of the system and to monitor phase stability during the course of the investigation. In all cases, the cubic-Ia3d or cubic-Pn3m phase were obtained (see Fig. 2).

2.4. NMR

High resolution ^{1}H NMR spectra were collected at 20 ± 0.2 °C on a Bruker DMX 600 MHz NMR spectrometer using a 5 mm triple resonance TXI probe with *xyz* gradients (Bruker). One or more X-ray capillaries containing the lipid sample were placed in a standard 5 mm thin-walled NMR tube (Wilmad Buena, NJ) containing D_2O (99.96%). Spectra were collected with and without spinning. Shimming typically took less than twenty minutes for the initial sample, and under 5 min for subsequent samples. ^{1}H spectra were collected with one pulse acquisition or WATERGATE solvent suppression [21,22].

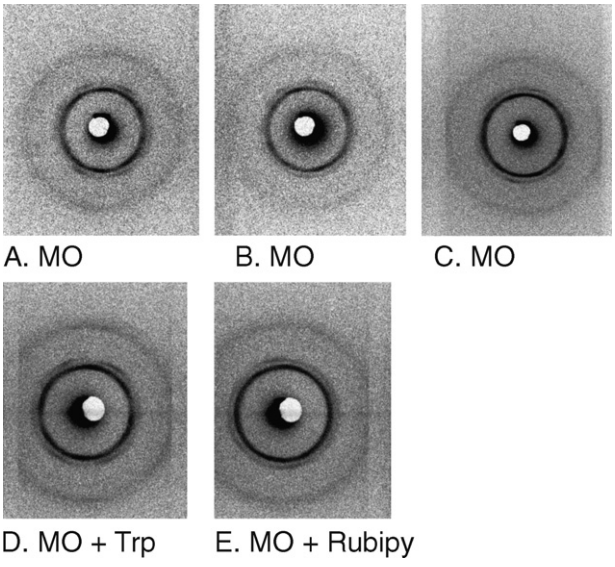

Fig. 2. Small-angle X-ray diffraction patterns of monolein/water samples in the cubic-Ia3d phase recorded at 20 °C. Sample were prepared at 37 %(w/w) hydration without additive (A–C), and with tryptophan (D) and rubipy (E) as described under Section 2. Measurements were made on fresh samples (A, B, D, E) and on a sample that was 2 months old (C). The lattice parameters for the different samples are 149 Å(A and B), 127 Å(C), 148 Å(D) and 146 Å(E).

3. Results and discussion

A critical first step in nearly all NMR studies is obtaining spectral resolution. With sufficient resolution resonances can be assigned, usually by exploiting isotropic chemical shifts and *J*-couplings. Once assignments are complete, dipolar couplings can be measured, often through cross-relaxation studies [23,24], and used to determine the presence of secondary and higher order structures. As mentioned in the Introduction, the lateral diffusion of molecules within the lipid bilayer of the cubic phase averages away all second rank NMR frequency anisotropies, resulting in high resolution spectra. Pampel and coworkers [13] had further shown that higher resolution ^{1}H NMR spectra of the monoolein cubic phase can be obtained using HR-MAS to remove the residual line broadenings from magnetic susceptibility variations. In Fig. 3 we show that the need for HR-MAS can be eliminated and that equivalent resolution can be obtained for the ^{1}H NMR spectrum of the cubic-Ia3d phase when the sample is carefully loaded in thin-walled glass capillaries. The 600 MHz ^{1}H NMR spectrum in Fig. 3 was obtained with 25 mg lipidic mesophase using a standard solution probe at 20 °C. Resonance assignments in this one-dimensional ^{1}H spectrum are given in Table 1. Because monoolein has a tendency to isomerize in aqueous dispersion producing an equilibrium mix of the 1- and 2-isomers (88% 1-monoolein and 12% 2-monoolein at 20 °C [25]),

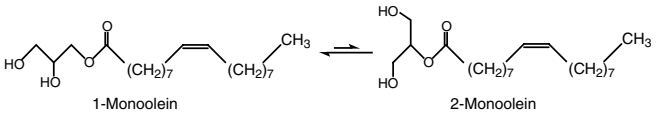

there are additional proton-OH resonances visible in the spectrum, near 3.7 ppm, due to the glycerol moiety of 2-monoolein. Monoolein chemical shifts were referenced by setting the terminal methyl group resonance (carbon number 18 in Fig. 3) to 0.900 ppm [13].

Shown in Fig. 4 is a portion of the *t*-ROESY [26] spectrum of the monoolein cubic-Ia3d phase loaded in a thin-walled capillary and measured using a standard solution probe at 20 °C. The ^{1}H spectrum has slightly higher resolution, as expected, compared the 500 MHz ^{1}H HR-MAS *t*-ROESY spectrum reported by Pampel and coworkers [13], as indicated by the resolution of crosspeaks between

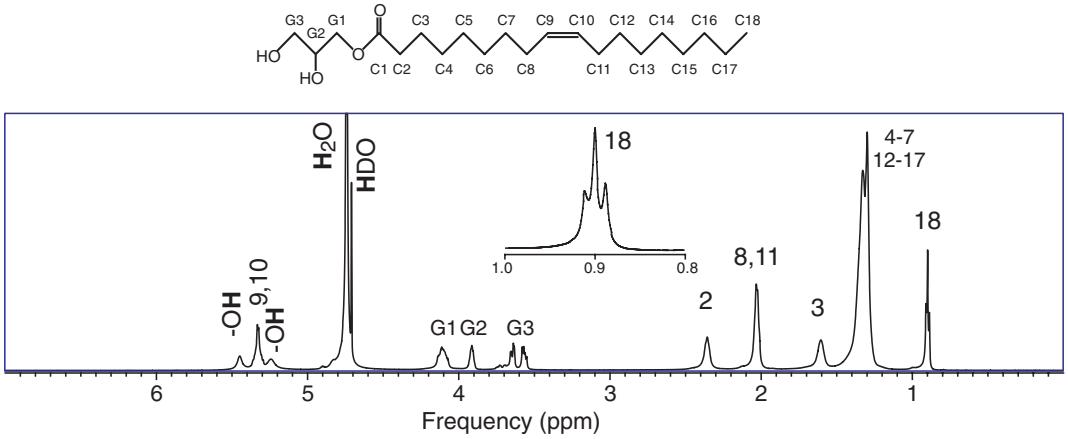

Fig. 3. ^{1}H NMR spectrum of the cubic-Ia3d phase formed by monoolein at 37%(w/w) water in a glass X-ray capillary. Data were collected on a 600 MHz spectrometer (8 KHz spectral width, 32k points, 128 acquisitions) at 20 °C without spinning. The spectrum was processed without apodization. The X-ray diffraction pattern of this sample is shown in Fig. 2C. The molecular structure of monoolein and the labeling used to identify resonances are shown at the top of the figure. A small amount of 2-monoolein is also present due to isomerization of 1-monoolein (see text). It gives rise to the additional resonances near 3.7 ppm.

Table 1
Proton chemical shift assignments and scalar J (indirect dipolar) couplings for resonances from monoolein in the lipidic cubic-Ia3d phase referenced to the terminal methyl of the oleoyl chain at 0.900 ppm

Hydrogen	ppm	Splitting	J_{HH} (Hz)
–(C**H**$_3$)	0.900	Triplet	6.7
–(C**H**$_2$)$_n$–	1.298		
	1.328		
–C**H**$_2$–CH$_2$COO–	1.605		
–C**H**$_2$CH=CH	2.012		
	2.023		
	2.033		
	2.043		
–C**H**$_2$COO–	2.356	Triplet	6.8
–**H**C=C**H**–	5.329		
1-MO:G3 –**H**CH–	3.557	Doublet	6.2
	3.576	Doublet	6.5
1-MO:G3 –HC**H**–	3.678	Doublet	5.7
	3.698	Doublet	4.5
1-MO:G2 –C**H**–	3.914	Quintet	4.7
1-MO:G1 –C**H**$_2$–	4.112		
1-MO:G1 and G2 –O**H**	5.243		
	5.449		
HDO in outer tube	4.710		
H$_2$O in cubic phase	4.742		

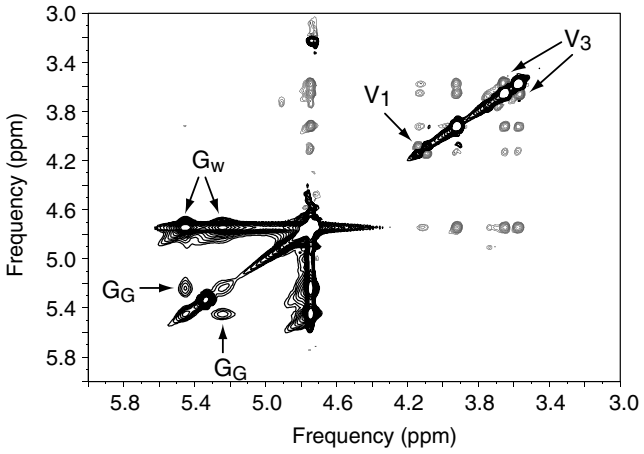

Fig. 4. Expanded view of the ^{1}H–^{1}H t-ROESY spectrum of the cubic-Ia3d phase recorded using monoolein at 37%(w/w) hydration in a glass capillary. Data were recorded on a 600 MHz spectrometer under the following conditions: pulse sequence, roesyph; sweep width, 1k × 512 points; 16 dummy scans; 8 acquisitions; 400 ms mixing time; 2500 Hz spin-lock field; 100 μs $\pi/2$ pulse. The spectrum reveals NOE crosspeaks between the vicinal hydrogens of the glycerol 1 and 3 –CH$_2$ groups, V_1 and V_3, respectively, and chemical exchange crosspeaks between the hydroxyl groups of glycerol, G_G, and between glycerol's hydroxyls and water, G_W.

the vicinal protons of the glycerol 1 and 3 –CH$_2$ groups, labeled V_1 and V_3, respectively. Additionally, the spectrum shows the chemical exchange of protons between the glycerol 1 and 3 –OH groups, labeled G_G, as well as between the glycerol –OH groups and water, labeled G_W.

3.1. Incorporation of L-tryptophan and rubipy

Previous work by one of us (MC) has shown that L-tryptophan and rubipy have essentially the same diffusion coefficients in bulk aqueous solution; however, the diffusion coefficient of L-tryptophan from the cubic phase is one fourth that of rubipy [4]. L-Tryptophan and rubipy are similar in size with calculated radii of gyration of 4.3 and 4.7 Å, respectively [4]. The longer release time for L-tryptophan from the cubic phase is attributed to molecular interaction with the lipid interface. We exploit our approach for obtaining high resolution NMR spectra in the cubic phase to explore and compare possible interactions of L-tryptophan and rubipy with the cubic lipid/aqueous interface.

Shown in Fig. 5 is a comparison of the ^{1}H NMR spectra of rubipy in aqueous solution and incorporated into the cubic phase at a 1:166 mol ratio. The ^{1}H NMR shift frequencies of rubipy are summarized in Table 2. Notice that there is a systematic average shift of $\sim 0.120 \pm 0.020$ ppm

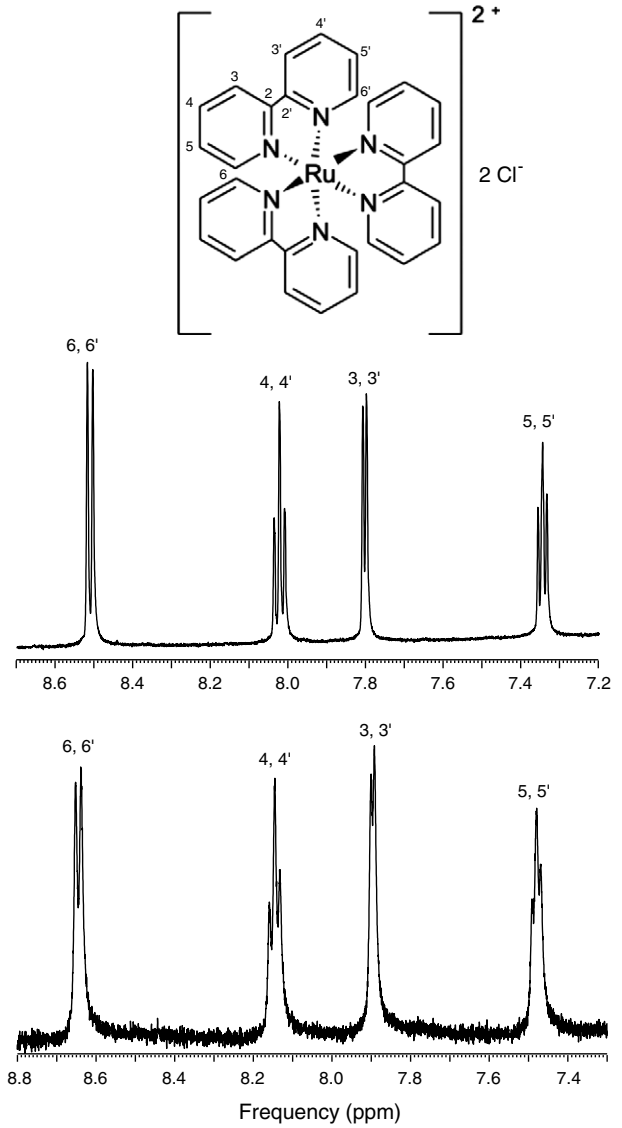

Fig. 5. ^{1}H NMR spectra of rubipy in bulk aqueous solution (upper panel) and incorporated into the cubic-Ia3d phase of monoolein at 37%(w/w) hydration (lower panel). Spectra were processed without apodization and were externally referenced to DSS. The concentration of rubipy in the aqueous solution was 10 mg/mL. The molecular structure of and proton identities in rubipy are shown in the upper panel. Individual resonances in the two spectra are labeled according to the molecular structure.

Table 2
NMR shift frequencies in ppm and scalar J (indirect dipolar) couplings of rubipy in aqueous solution and incorporated in the cubic phase

Site	Splitting	Aqueous phase		Cubic phase		$\Delta\delta$ (ppm)
		δ_w (ppm)	J (Hz)	δ_{cp} (ppm)	J (Hz)	
3,3′	Doublet	7.805	5.81	7.897	5.57	0.092
4,4′	Triplet	8.024	8.37	8.146	8.31	0.122
5,5′	Triplet	7.346	7.06	7.479	6.86	0.133
6,6′	Doublet	8.512	8.67	8.645	8.64	0.133

The shift difference is calculated according to $\Delta\delta = \delta_{cp} - \delta_w$. Site refers to proton location in rubipy as defined in the molecular structure shown in Fig. 5.

in all resonances. Additionally, there is a uniform 2–3 Hz increase in linewidth upon incorporation into the cubic mesophase, which likely arises from residual bulk magnetic susceptibility variations in the sample. Generally, there are two contributions to the observed NMR shift: (i) the bulk magnetic susceptibility of the phase, which causes a systematic average shift of all the protons on a molecule in that phase [27] and (ii) the local susceptibility, i.e., the chemical shift, which is sensitive to changes in the local environment. While the absolute NMR shift of the rubipy resonances are different in bulk water and cubic phase, the NMR (chemical shift) difference between each proton resonance is essentially the same in water as it is in the cubic phase. This indicates that changes in the NMR shift arise primarily from bulk susceptibility changes and not as a result of differential specific molecular-level interactions. This is consistent with release studies [4] which show that rubipy remains in the aqueous channel of cubic phase and that it does not partition at or interact with the interface.

In Fig. 6 is a comparison of the ^{1}H NMR spectra of the indole region of L-tryptophan in aqueous solution and incorporated into the cubic phase at a 1:122 mol ratio. The ^{1}H NMR shift frequencies are summarized in Table 3. As with rubipy, both a change in absolute NMR shift and linewidth of L-tryptophan resonances is observed. In contrast to rubipy, however, there are significant changes in the chemical shift differences amongst protons in L-tryptophan upon changing from bulk water to the cubic phase. That is, the differences in NMR shifts of L-tryptophan arise

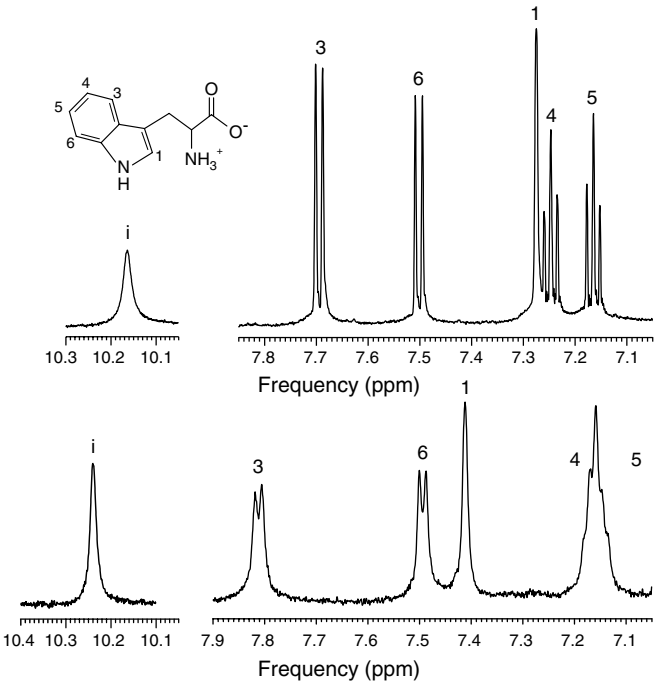

Fig. 6. Downfield region of the ^{1}H NMR spectra of L-tryptophan in bulk aqueous solution (upper panel) and in the cubic-Ia3d phase of monoolein at 37%(w/w) water (lower panel). Spectra were processed without apodization and externally referenced to DSS. The concentration of tryptophan in the aqueous solution was 8 mg/mL.

Table 3
NMR shift frequencies in ppm and scalar J (indirect dipolar) couplings of L-tryptophan in aqueous solution and incorporated in the cubic phase

Site	Splitting	Aqueous phase		Cubic phase		$\Delta\delta$ (ppm)	$\Delta\delta'$ (ppm)
		δ_w (ppm)	J (Hz)	δ_{cp} (ppm)	J (Hz)		
i	Singlet	10.168	—	10.240	—	0.072	−0.048
1	Singlet	7.278	—	7.412	—	0.134	0.014
3	Doublet	7.698	8.16	7.812	8.21	0.114	−0.006
4	Triplet	7.250	7.63	7.159	7.45	−0.091	−0.211
5	Triplet	7.167	7.58	7.159	7.45	−0.008	−0.128
6	Doublet	7.505	8.25	7.495	7.85	−0.010	−0.130

The shift differences are calculated according to $\Delta\delta = \delta_{cp} - \delta_w$ and $\Delta\delta' = \Delta\delta - \langle\Delta\delta\rangle_{rubipy}$ where $\langle\Delta\delta\rangle_{rubipy} = 0.12 \pm 0.02$ ppm. Site refers to proton location in L-tryptophan as defined in the molecular structure shown in Fig. 6.

as a result of both bulk susceptibility changes and differential specific molecular-level interactions. Although we cannot cleanly separate the sources behind the shift differences of L-tryptophan, we can use rubipy as a control for the average shift difference due to bulk susceptibility differences of the two phases. Subtracting the average $\Delta\delta$ for rubipy of 0.12 ± 0.02 ppm, we obtain the adjusted $\Delta\delta'$ values for each L-tryptophan site also given in Table 3. Generally, an upfield, or positive chemical shift difference is associated with exposure to a more polar or solvated environment [28,29]. Conversely, a negative chemical shift change results from movement towards a less polar or less solvated environment. The large negative chemical shift changes observed at sites 4, 5, and 6 when L-tryptophan is incorporated into the cubic phase is consistent with L-tryptophan being partially inserted into the bilayer interface and shielded from water [29].

Additionally, we note that the linewidth of the indole ring resonances increased by 3–6 Hz in the cubic phase compared to bulk aqueous solution, except in the case of the –NH proton (peak i in Fig. 6), where the linewidth decreased by almost 5 Hz. Generally, the indole–NH proton linewidth in bulk water is broadened, compared to the other proton resonances in L-tryptophan, due to proton exchange with water [30]. The decrease in the indole–NH proton resonance in going from bulk to mesophase implies a decrease in this exchange rate. Such a decrease could arise from an increased micro-viscosity of water in the channels of the cubic phase, or from L-tryptophan having more specific interactions with the bilayer interface, or both. Further work is needed to distinguish between these possibilities. Overall, our results are in agreement with separate transport and spectroscopic studies performed on the cubic phase [4,3,31,32]; and with current studies of L-tryptophan analogs in the interfacial region of phospholipid bilayers [33,34].

4. Summary

We have shown that high resolution ^{1}H NMR spectra with resolved J-coupling multiplets of the cubic phase of monoolein can be obtained using a conventional liquid state NMR probe and without HR-MAS, by carefully loading uniform and homogenous samples of the high viscosity cubic phase into thin-walled glass capillaries. Additionally, we have illustrated with L-tryptophan and rubipy that the kind of high resolution NMR spectra attainable in the cubic phase can be a useful tool to probe specific molecular interactions of additive molecules with lipid bilayers. Overall, the combination of the cubic phase and NMR could provide a valuable complement to other NMR approaches, such as oriented lipid bilayers on glass slides [35,36], MAS applied to multilamellar vesicles [37–39], or bicelles [40], for investigating structure and dynamics in model membrane systems.

Acknowledgments

The authors thank Profs. Chris Jaroniec and Tom Barbara for insightful comments and advice, and Dr. Chunhua Yuan for technical assistance. Supported in part by Science Foundation Ireland (02-IN1-B266), the National Institutes of Health (GM61070, GM075915), and the National Science Foundation (DIR9016683 and DBI9981990) to M.C. and the National Science Foundation under Grant No. CHE-0616881 to P.J.G. Any opinions, findings and conclusions or recommendations expressed in this material are those of the author(s) and do not necessarily reflect the views of the National Science Foundation (NSF).

References

[1] E.M. Landau, J.P. Rosenbusch, Lipic cubic phases: a novel concept for the crystallization of membrane proteins, Proc. Natl. Acad. Sci. USA 93 (1996) 14532–14535.
[2] M. Caffrey, Membrane protein crystallization, J. Struct. Biol. 142 (1) (2003) 108–132.
[3] J. Clogston, G. Craciun, D.J. Hart, M. Caffrey, Controlling release from the lipidic cubic phase by selective alkylation, J. Cont. Rel. 102 (2) (2005) 441–461.
[4] J. Clogston, M. Caffrey, Controlling release from the lipidic cubic phase, amino acids, peptides, proteins and nucleic acids, J. Cont. Rel. 107 (2005) 97–111.
[5] D.P. Siegel, V. Cherezov, D.V. Greathouse, R.E. Koeppe II, J.A. Killian, M. Caffrey, Transmembrane peptides stabilize inverted cubic phases in a biphasic length-dependent manner: Implications for protein-induced membrane fusion, Biophys. J. 90 (2006) 200–211.
[6] J.S. Patton, M.C. Carey, Watching fat digestion, Science 204 (1979) 145–148.
[7] D.M. Anderson, S.M. Gruner, S. Leibler, Geometrical aspects of the frustration in the cubic phases of lyotropic liquid crystals, Proc. Natl. Acad. Sci. USA 85 (1988) 5364–5368.
[8] S. Hyde, S. Andersson, K. Larsson, Z. Blum, T. Landh, S. Lidin, B. Ninham, The Language of Shape, Elsevier Science, 1996.
[9] A. Samoson, B.Q. Sun, A. Pines, New angles in motional averagingPulsed Magnetic Resonance: NMR, ESR, and Optics—A recognition of E.L. Hahn, Clarendon Press, Oxford, 1992.
[10] G. Lindblom, L. Rilfors, Cubic phases and isotropic structures formed by membrane lipids-possible biological relevance, Biochim. Biophys. Acta 988 (1989) 221–256.
[11] P.R. Cullis, B.d. Kruijff, Polymorphic phase behaviour of lipid mixtures as directed by ^{31}P NMR, Biochim. Biophys. Acta 507 (1978) 207–218.

[12] P.R. Cullis, M.J. Hope, Effects of fusogenic agents on membrane structure of erythrocyte ghosts and the mechanism of membrane fusion, Nature 271 (1978) 672–674.
[13] A. Pampel, E. Strandberg, G. Lindblom, F. Volke, High-resolution NMR on cubic lyotropic liquid crystalline phases, Chem. Phys. Lett. 287 (1998) 468–474.
[14] C. Glaubitz, A. Watts, Magic angle-oriented sample spinning (maoss): a new approach toward biomembrane studies, J. Magn. Reson. 130 (1998) 305–316.
[15] A. Pampel, K. Zick, H. Glauner, F. Engelke, Studying lateral diffusion in lipid bilayers by combining a magic angle spinning NMR probe with a microimaging gradient system, J. Am. Chem. Soc. 126 (2004) 9534–9535.
[16] A. Pampel, D. Michel, R. Reszka, Pulsed field gradient MAS-NMR studies of the mobility of carboplatin in cubic liquid-crystalline phases, Chem. Phys. Lett. 357 (2002) 131–136.
[17] T.M. Barbara, Cylindrical demagnetization fields and microprobe design in high-resolution NMR, J. Magn. Reson. A 109 (1994) 265–269.
[18] D. Edmonds, M. Wormald, Theory of resonance in magnetically inhomogeneous specimens and some useful calculations, J. Magn. Reson. 77 (1988) 223–232.
[19] A. Cheng, B. Hummel, H. Qui, M. Caffrey, A simple mechanical mixer for small viscous lipid-containing samples, Chem. Phys. Lett. 95 (1998) 11–21.
[20] H. Qiu, M. Caffrey, The phase diagram of the monoolein/water system: metastability and equilibrium aspects, Biomaterials 21 (2000) 223–234.
[21] M. Piotto, V. Saudek, V. Sklenar, Gradient-tailored excitation for single-quantum nmr spectroscopy of aqueous solutions, J. Biomol. NMR 2 (6) (1992) 661–665.
[22] T.-L. Hwang, A.J. Shaka, Water suppression that works excitation sculpting using arbitrary waveforms and pulsed field gradients, J. Magn. Reson. A 112 (1995) 275–279.
[23] D. Neuhaus, M.P. Williamson, The Nuclear Overhauser Effect in Structural and Conformational Analysis, Weinheim, New York, 1989.
[24] K. Wüthrich, NMR of Proteins and Nucleic Acids, Wiley, 1986.
[25] H. Ljusberg-Wahren, M. Herslöf, K. Larsson, A comparison of the phase behaviour of the monoolein isomers in excess water, Chem. Phys. Lipids 33 (1983) 211–214.
[26] T.-L. Hwang, A.J. Shaka, Cross relaxation with TOCSY: transverse rotating-frame overhauser effect spectroscopy, J. Am. Chem. Soc. 114 (1992) 3157–3159.
[27] A. Abragam, Principles of Nuclear Magnetism, Oxford University Press, Walton Street, Oxford OX2 6DP, 1961.
[28] J.A. Hamilton, D.M. Small, Solubilization and localization of triolein in phosphatidylcholine bilayers: a ^{13}C NMR study, Proc. Natl. Acad. Sci. USA 78 (11) (1981) 6878–6882.
[29] U.R.K. Rao, C. Manohar, B.S. Valaulikar, R.M. Iyer, Micellar chain model for the origin of the visoelasticity in dilute surfactant solutions, J. Phys. Chem. 91 (12) (1987) 3286–3291.
[30] A. Carrington, A.D. McLachlan, Introduction to Magnetic Resonance, Chapman and Hall, Methuen, Inc., 1967.
[31] J. Kim, W. Lu, W. Qiu, L. Wang, M. Caffrey, D. Zhong, Ultrafast hydration dynamics in the lipidic cubic phase: discrete water structures in nanochannels, J. Phys. Chem. B 110 (2006) 21994–22000.
[32] W. Liu, M. Caffrey, Interactions of tryptophan, tryptophan peptides and tryptophan alkyl esters at curved membrane interfaces, Biochemistry 45 (2006) 11713–11726.
[33] S. Persson, J.A. Killian, G. Lindblom, Molecular ordering of interfacially localized tryptophan analogs in ester- and ether-lipid bilayers studied by H-2-NMR, Biophys. J. 75 (3) (1998) 1365–1371.
[34] W.-M. Yau, W.C. Wimley, K. Gawrisch, S.H. White, The preference of tryptophan for membrane interfaces, Biochemistry 37 (42) (1998) 14713–14718.
[35] R.R. Ketchem, W. Hu, T.A. Cross, High-resolution conformation of gramicidin a in a lipid bilayer by solid-state NMR, Science 261 (1993) 1457–1460.
[36] S.J. Opella, F.M. Marassi, Structure determination of membrane proteins by NMR spectroscopy, Chem. Rev. 104 (2004) 3587–3606.
[37] F. Caboi, J. Borne, T. Nylander, A. Khan, A. Svendsen, S. Patkar, Lipase action on a monoolein/sodium oleate aqueous cubic liquid crystalline phase—a NMR and X-ray diffraction study, Coll. Sur. B-Biointerfaces 26 (1–2) (2002) 159–171.
[38] E. Oldfield, J.L. Bowers, J. Forbes, High-resolution proton and carbon-13 NMR of membranes: Why sonicate? Biochemistry 26 (1987) 6919–6923.
[39] E.G. Finer, A.G. Flook, H. Hauser, The nature and origin of the NMR spectrum of unsonicated and sonicated aqueous egg yolk lecithin dispersions, Biochim. Biophys. Acta 260 (1) (1972) 59–69.
[40] R.R. Vold, R.S. Prosser, A.J. Deese, Isotropic solutions of phospholipid bicelles: a new membrane mimetic for high-resolution NMR studies of polypeptides, J. Biomol. NMR 9 (1997) 329–335.